Available online at www.sciencedirect.com

ScienceDirect

Physics Procedia 61 (2015) 443 – 449

Physics Procedia

Measuring the cosmic ray energy spectrum and composition with IceCube

B. Ruzybayev for the IceCube Collaboration[a,1]

[a] *University of Delaware, Newark, Delaware, USA, 19716*

Abstract

We report a measurement of the all-particle cosmic ray energy spectrum with IceCube. The results of two different techniques are discussed. The first result is a measurement of the all-particle cosmic ray energy spectrum in the energy range from 1.58 PeV to 1.26 EeV using the IceTop air shower array, which is the surface component of the IceCube Neutrino Observatory at the South Pole. The second result is a measurement of both cosmic ray energy spectrum and composition using neural network techniques and the full IceCube as a 3-dimensional cosmic ray detector. The measured energy spectrum exhibits clear deviations from a single power law above the knee around 4 PeV and below 1 EeV.

Selection and peer review is the responsibility of the Conference lead organizers, Frank Avignone, University of South Carolina, and Wick Haxton, University of California, Berkeley, and Lawrence Berkeley Laboratory

Keywords: IceCube, Spectrum

1. Introduction

For improved understanding of the acceleration and propagation of high energy cosmic rays, high resolution measurements of the cosmic ray energy spectrum and elemental composition are needed. The IceCube Neutrino Observatory [1] is ideally suited to measure both the energy spectrum and chemical composition of the primary cosmic rays. IceCube detects the electromagnetic component of air showers with the surface array and the high energy muonic component with the deep ice detectors. IceCube is a cubic-kilometer neutrino detector consisting of 86 deep strings and 81 surface stations in the final configuration. The inter-station and inter-string separation is about 125 m. Each deep string contains 60 Digital Optical Modules (DOMs) [1] positioned between depths of 1450 m to 2450 m. The surface stations comprise the IceTop air shower array [2]. Each surface station consists of two ice-Cherenkov tanks separated by 10 m. Two DOMs are deployed per tank. Each DOM contains a 10 inch photomultiplier tube (PMT) and electronics for signal processing and readout [3].

2. Data and Simulation

The analyses that we are reporting here used data taken between June 1, 2010 to May 13, 2011, when IceCube consisted of 79 strings and 73 surface stations. The effective live-times, depending on the analysis and selection criteria, were 327 for IceTop only and 310 days for coincident analysis.

[1] http://www.icecube.wisc.edu

Selection and peer review is the responsibility of the Conference lead organizers, Frank Avignone, University of South Carolina, and Wick Haxton, University of California, Berkeley, and Lawrence Berkeley Laboratory

doi:10.1016/j.phpro.2014.12.106

Detailed simulations were used to relate the measured air shower parameters to properties of the primary cosmic rays. Air showers were simulated in a wide energy range from 10^5 GeV to $10^{9.5}$ GeV with CORSIKA [4]. Showers above 10^8 GeV were 'thinned' [5] to reduce computational time and storage volume. Hadronic interaction models used were SIBYLL 2.1 [6] for interactions with energies greater than 80 GeV and FLUKA [7] at lower energies. A smaller set was simulated using QGSJET-II [8] for systematic studies. The simulated atmosphere had an atmospheric overburden of 692.9 g/cm^2 (680 hPa), which is also the average overburden for the full year of data. Snow cover on top of the tanks in the simulation was that measured in February 2010. Air showers were simulated with equal numbers of showers per $\sin\theta\cos\theta$ bin, in a zenith range of 0 to 40 degrees. Four primary types, H, He, O, Fe, were simulated with more than 42000 CORSIKA showers per primary. During the analysis, showers are reweighted with different assumed spectra. Each CORSIKA shower was resampled 100 times to increase statistics. Shower cores were uniformly distributed over areas larger than the detector area with an energy dependent resampling radius. The detector response was simulated using IceCube software that simulates the entire chain of data taking and hardware [2]. Interactions of charged particles with the IceTop tanks were simulated using the GEANT4 [9] package.

3. Surface only - IceTop analysis

The IceTop reconstruction algorithm [2] uses information from individual tanks, including location, charge and pulse time. The measured charges are fitted with a Lateral Distribution Function (LDF):

$$S(R) = S_{ref}\left(\frac{R}{R_{ref}}\right)^{-\beta-0.303\log_{10}\left(\frac{R}{R_{ref}}\right)}, \tag{1}$$

while signal times are fitted with a function describing the geometric shape of the shower front. From these fits, shower direction, core location and shower size are reconstructed. S_{ref} in LDF is the shower size or signal at a reference distance R_{ref} perpendicular to the shower axis and β is the slope of the logarithmic LDF at R_{ref}. The shower size, S_{125}, is defined as the fitted value of the LDF (Eq.1) at a perpendicular distance of 125 m away from the shower axis. Since IceTop is located at the geographic South Pole, snow accumulates on top of IceTop tanks with time, which reduces the measured signal in a tank. As a result, a correction [10] is applied that reduces the expected signal in the likelihood fitting procedure on a tank by tank basis. The core resolution of the surface reconstruction method is better than 15 m around a few PeV and improves to less than 8 m at higher energy. The directional resolution is between $0.2^\circ - 0.8^\circ$, depending on energy and zenith angle. Only well contained events that passed basic quality cuts, with at least 5 stations triggered and with a reconstructed $\cos\theta \geq 0.8$ were selected for this analysis. Since coincidence with the deep ice detector was not required, the statistics are higher for the surface-only analysis.

To estimate the energy of the primary cosmic ray with the surface detector, the relationship between the shower size S_{125} and the true primary energy, E_{true}, is derived from simulations [10]. This relationship depends on the mass of the primary particle and the zenith angle of the air shower. Figure 1 shows a 2-dimensional histogram of the $\log_{10}(S_{125})$ vs $\log_{10}(E_{true})$ for simulated protons weighted by a flux model $\frac{dN}{dE} \propto E^{-2.7}$. Similar distributions to Figure 1 can be made for various assumptions about the primary cosmic ray composition. For each assumed composition, this relationship is parametrized with a linear function obtained by calculating the mean primary energy for each bin in measured S_{125}. In this way the primary energy is estimated for a given zenith range and primary assumption [10]. The final spectrum was derived assuming a mixed composition called the H4a model [11]. Figure 2 shows the relations between primary energy and S_{125} at four zenith angles for a mixed composition assumption.

The final spectrum was derived assuming the H4a model and averaged over the full zenith range $\cos\theta \geq 0.8$. There are four major systematic uncertainties in the energy estimation that were accounted for in this analysis: 1) uncertainty in the VEM calibration that results in a 3% uncertainty in the absolute energy scale, 2) uncertainty in snow correction which affects the estimated detector signal, 3) difference between SYBILL 2.1 and QGSJET II, and 4) uncertainty due to composition dependence.

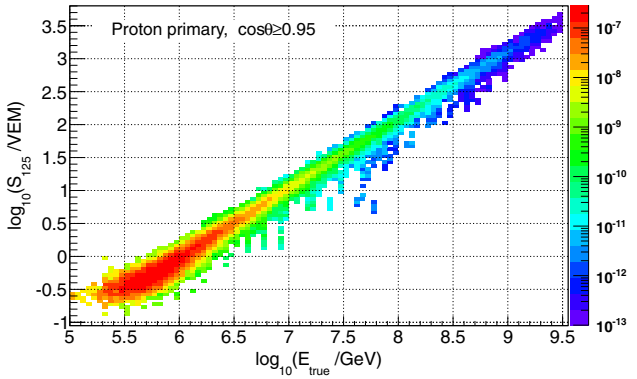

Fig. 1. $\log_{10}(S_{125})$ vs. $\log_{10}(E_{true})$ scatter plot for proton primary simulation with $\cos\theta \geq 0.95$, weighted by a flux model $\frac{dN}{dE} \propto E^{-2.7}$

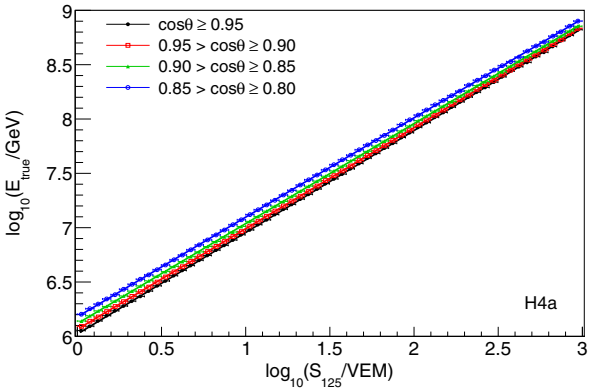

Fig. 2. S_{125}-to-E_{true} relations in four zenith ranges for the H4a composition assumption.

The method used in this analysis requires a predefined composition assumption to translate the measured S_{125} spectrum to the primary energy spectrum. In addition to the baseline scenario, the mixed composition H4a, we considered 4 extreme composition assumptions (pure proton, pure helium, pure oxygen and pure iron), to estimate the impact of the composition uncertainties on the all-particle spectrum.

Assuming that the cosmic ray directions are isotropically distributed, the measurement of the spectrum in different zenith ranges should yield the same result for each zenith. For a given energy, protons or light nuclei penetrate deeper into the atmosphere compared to heavy nuclei like iron. Heavy nuclei start to interact higher in the atmosphere and showers will be at a different stage of development at the detector level compared to light nuclei. When looking at large zenith angle events, one effectively increases the amount of atmosphere that showers need to traverse to get to the detector. This information is sensitive to composition.

Reconstruction of the experimental data assuming pure proton and pure iron compositions in four zenith ranges are shown in Figures 3(a) and 3(b). It can be seen that for a pure proton assumption the most inclined spectrum ($0.80 \leq \cos\theta < 0.85$) is systematically lower than vertical spectrum ($\cos\theta \geq 0.95$), in the energy range where statistics are not an issue. While for the pure iron assumption it is the opposite, the inclined spectrum is systematically higher than the vertical.

Four zenith spectra for the mixed H4a composition assumption can be seen in Figure 3(c). Compared to pure proton and pure iron, the H4a assumption leads to a smaller difference between vertical and inclined spectra, but still not zero. The largest difference between spectra is taken as a fixed value for the systematic error due to composition across all energies as a conservative estimate.

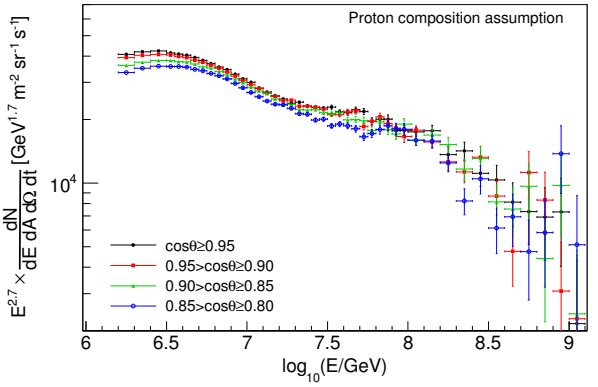

(a) Proton.

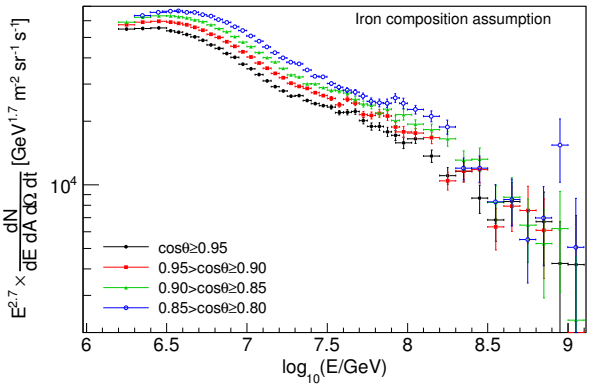

(b) Iron.

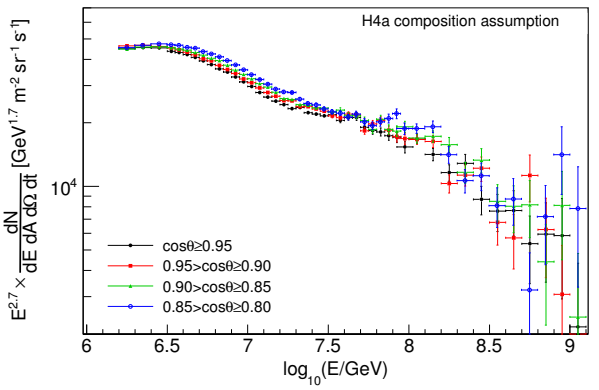

(c) H4a.

Fig. 3. Cosmic ray energy spectrum for 3 composition assumptions and 4 zenith ranges.

4. Coincident analysis

The coincident analysis uses both surface detector and the deep ice detector measurements. The signal in the deep ice detector in coincident events is due to collimated bundles of up to thousands of high energy muons. The deep ice detector detects the Cherenkov light emitted by these high energy (TeV) muon bundles

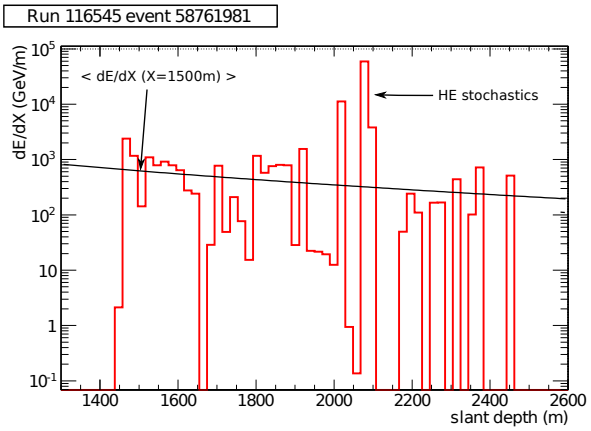

Fig. 4. Muon bundle energy loss reconstruction for one event of about 200 PeV.

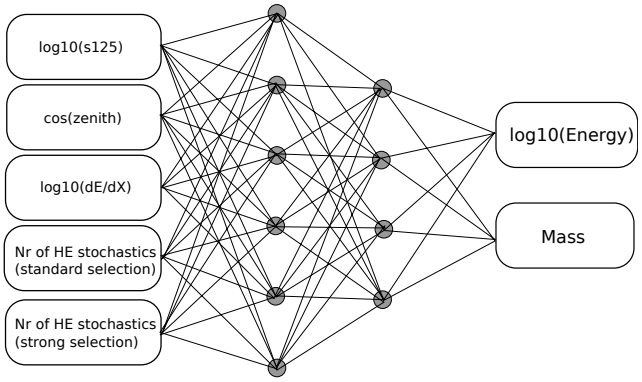

Fig. 5. The 5-6-4-2 network used in the coincident analysis. Five input variables are mapped to two output variables, primary mass and energy.

as they lose energy through ionization and radiative processes. Using the amplitude and timing measured by DOMs in the deep ice, the energy loss profile of these bundles is reconstructed using an unfolding procedure [12]. The example of this energy loss profile on Figure 4 shows the stochastic behavior of a large event.

The muon bundle energy loss at a fixed slant depth is highly dependent on the muon bundle multiplicity and consequently, composition. In addition, the stochastic behavior is also composition dependent since the probability of several muons giving a radiative energy loss on the same track segment is higher for iron, which has higher multiplicity, compared to proton. The coincident analysis uses two selection criteria, one stronger and one weaker, for counting stochastic losses [12]. For the coincident analysis, in addition to passing basic quality cuts on the reconstruction, the event must be well contained by the surface array. Random coincident events, that is two separate air showers that trigger both the deep ice detector and surface array in the same time frame, are removed using timing information.

The coincident analysis reconstructs both mass and energy of the primary cosmic ray using a multilayer perceptron neural network (NN) [12]. The five primary mass and energy sensitive observables used as NN inputs are the surface shower size S_{125}, the average energy loss at a fixed slant depth of 1500 m (dE/dX), the zenith angle, and numbers of high energy stochastics using two different selection criteria [12]. Figure 5 shows the neural network used in this analysis. Unlike the surface-only analysis, the coincident analysis reconstructs both primary mass and energy. As a result, the energy spectrum does not have an explicit dependence on composition.

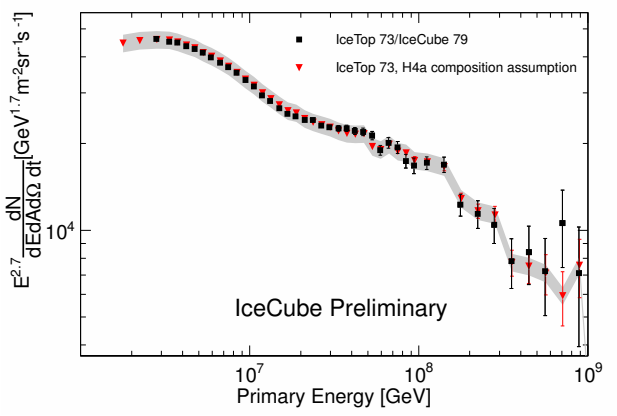

Fig. 6. The differential energy spectra for both the coincident and surface-only analyses. The shaded area represents the systematic uncertainty due to composition for the surface-only analysis.

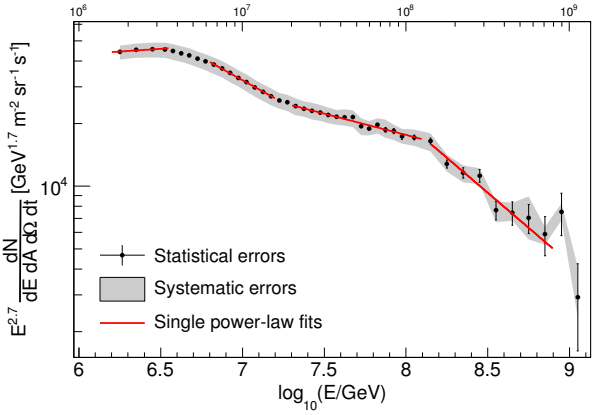

Fig. 7. Spectral fits in different energy ranges. Shaded area represents the systematic errors added in quadrature.

5. Results and discussion

The final spectra from both analyses are shown in Figure 6. Both spectra agree well within the compositional uncertainty of the surface-only analysis. The spectrum from the surface-only analysis was derived using shower size (S_{125}) to energy parametrization calibrated using the H4a composition model assumption. We observe that, beyond our systematics, the all-particle cosmic-ray energy spectrum does not follow a single power law above the knee (4.4 ± 0.4 PeV), but shows significant structure. The final spectrum from the surface-only analysis was fitted by a simple power function of the form

$$\frac{\mathrm{d}N}{\mathrm{d}\ln E\,\mathrm{d}A\,\mathrm{d}\Omega\,\mathrm{d}t} = I_0\left(\frac{E}{1\,\mathrm{GeV}}\right)^{-\gamma+1}, \tag{2}$$

in four different energy ranges. The spectral index before the knee is $-2.63 \pm 0.01 \pm 0.06$, and changes smoothly between 4 to 7 PeV to $-3.13 \pm 0.01 \pm 0.03$. Another break is observed at around 18 ± 2 PeV, above which the spectrum hardens with a spectral index of $-2.91 \pm 0.01 \pm 0.03$. A sharp fall is observed beyond 130 ± 30 PeV with a spectral index of $-3.37 \pm 0.08 \pm 0.08$. Figure 7 shows the power function fits to the spectrum.

In summary, we have obtained measurements of the cosmic-ray energy spectrum with two different techniques. The hardening of the spectrum around 18 PeV and steepening around 130 PeV is a clear signature of

the spectrum and cannot be attributed to any of the systematics or detector artefacts. The preliminary result from the coincident analysis [12] shows that the composition becomes increasingly heavy up to 100 PeV.

References

[1] R.Abbasi et al., The IceCube Data Acquisition System: Signal Capture, Digitization, and Timestamping, Nucl. Instrum. Meth. A 601, (2009) 294-316
[2] R.Abbasi et al., IceTop: The surface component of Icecube, Nucl. Instrum. Meth. A 700 (2013) 188-220
[3] R.Abbasi et al., Calibration and Characterization of the IceCube Photomultiplier Tube, Nucl. Instrum. Meth. A 618 (2010) 139-152
[4] D.Heck et al., CORSIKA: A Monte Carlo code to simulate extensive air showers, report FZKA 6019 (1998)
[5] D.Heck, T.Pierog, Extensive Air Shower Simulation with CORSIKA: A User's Guide, `http://www-ik.fzk.de/corsika/usersguide/corsika_tech.html`
[6] E.Ahn et al., Cosmic ray interaction event generator SIBYLL 2.1, Phys. Rev. D80 (2009) doi:10.1103/PhysRevD.80.094003
[7] G.Battistoni et al., The FLUKA code: Description and benchmarking, in: Proceedings of the AIP 2007, 896, 31-49
[8] S.Ostapchenko, QGSJET-II: towards reliable description of very high energy hadronic interactions, Nucl. Phys. B Proc. Suppl 151 (2006) 143-146
[9] S.Agostinelli et al, GEANT4: A simulation Tool Kit, Nucl. Instrum. Meth. A 506 (2003) 250-303
[10] M.G.Aartsen et al., Measurement of the cosmic ray energy spectrum with IceTop-73, Phys. Rev. D88 (2013), doi:http://dx.doi.org/10.1103/PhysRevD.88.042004
[11] T.K.Gaisser, Spectrum of cosmic-ray nucleons, kaon production, and the atmospheric muon charge ratio, Astropart. Phys. 35 (2012) 801-806
[12] Tom Feusels, Katherine Rawlins for the IceCube collaboration, Cosmic Ray Composition and Energy Spectrum between 2.5 PeV and 1 EeV with IceTop and IceCube, in: Proceedings of the 33^{rd} ICRC 2013, Rio de Janeiro, Brazil